

# Computational Fluid Dynamics Analysis Procedure and Genetic Algorithm Application for Evaluating Performance of Double Pipe Heat Exchanger

Dina Sami Kadhim<sup>1\*</sup>, Samira Ahmed Assi<sup>1</sup>, Jamela Saadi Aziz<sup>1</sup>, Zahraa Ahmed Nadeem<sup>2</sup>

<sup>1</sup> Basra Engineering Technical College, Southern Technical University, Basra, Iraq

<sup>2</sup> Shatt Al-Arab University College, Basra, Iraq

\* Corresponding author's e-mail: dina.sami@stu.edu.iq

## ABSTRACT

For the time being, there is a growing endeavor towards supporting energy-saving technologies, most significantly heat exchanger systems, by improving the performance of the heat transfer process. The study model employed is a double-pipe heat exchanger (DPHEX), which is served in an actual project at the Low-Density Polyethylene (LDPE) unit of the State Company for Petrochemical Industries in Basra, Iraq. The prominent goals of this study are to gain a deeper comprehension of the exchanger's performance under advanced operating conditions and to maximize the efficiency of heat transfer between the two fluids in the DPHEX system. The current work applies a distinctive connection of SOLIDWORKS with ANSYS FLUENT software to conduct a simulation design and computational fluid dynamics (CFD) analysis of a heat transfer system in DPHEX. Thermal analysis of exchangers is challenging since many parameters, such as the geometry of the heat exchangers and the varying flow regimes influence the overall heat transfer coefficient. As a result, a Genetic Algorithm (GA) was employed to investigate the optimal design and operating conditions of DPHEX, using a COM server to provide flexible communication between the MATLAB GA toolbox and Aspen HYSYS<sup>®</sup> software. The preliminary findings from ANSYS FLUENT simulations and GA optimizations demonstrated significant improvements. Specifically, the heat transfer rate rose by 24% and 28%, respectively, also there made up an elevate in the overall heat transfer coefficient to 675 W/m<sup>2</sup>·K and 751 W/m<sup>2</sup>·K, correspondingly, from 440 W/m<sup>2</sup>·K in the as-built heat exchanger. Notably, these results were observed while the outgoing temperature of the chilled ethylene gas was at 49 °C, and the efficiency accounted for 87.7%. The study exhibited the feasibility of reducing the cooling water quantity from the traditional mass flow rate of 73.860 kg/hr to 50.400 kg/hr while maintaining a reasonable efficiency of 83% at the LDPE unit. These results were achieved with the leaving temperature of ethylene gas and cooling water set at 50 °C and 34 °C, respectively. Hence, minimizing water consumption in heat exchangers brings about environmental, economic, and operational advantages. Generally, the study results have reinforced the importance of simulation tools and their direct contribution to achieving efficient and eco-friendly energy systems.

**Keywords:** DPHEX, ANSYS FLUENT, CFD, genetic algorithm, heat transfer coefficient.

## INTRODUCTION

Heat exchangers are engineering apparatuses designed to efficiently transfer heat between two fluids without mixing them. Heat exchangers play a crucial role in energy conservation by extracting heat from a system that does not require it and transferring it to another system where it can be utilized. Heat exchangers come in various forms

and types, categorized based on factors such as design, construction, space requirements, fluid flow system, and the number of fluids involved in the heat transfer process. One commonly used type is DPHEX, as depicted in Figure 1. DPHEX is further classified into two basic types: counter flow and parallel flow, with the flow direction impacting the heat transfer rate and pressure drop in the system. This classification serves as the



**Figure 1.** DPHEX in industrial applications [5]

foundation for designing the heat exchanger, determining its size, length, and the number of bends required [1]. DPHEX operates based on a design where a smaller tube is contained within a larger tube in a concentric arrangement. The heat transfer process occurs within the larger tube, while the smaller tube serves as a connecting spacer. This configuration is often referred to as a jacketed U-exchanger and can feature either a single tube or multiple tubes. In this setup, one fluid flows through the inner tube while the other fluid flows between the two tubes. It is recommended to have the more viscous fluid on the outer shell side to take advantage of the increased flow area. The counterflow configuration is typically preferred for DPHEX design. This is because it offers optimal heat transfer coefficients, allowing the cold fluid to achieve a higher exit temperature than the hot fluid. In contrast, the parallel flow configuration yields lower heat transfer and reduced efficiency. However, there are specific applications where a parallel flow heat exchanger may be chosen despite its lower efficiency, as it serves unique requirements or constraints [2]. DPHEXs yield a high heat transfer coefficient and can endure harsh conditions, such as high pressures, making them well-suited for demanding applications. However, the limitations of DPHEXs include challenges in transportation due to their large size and results in high manufacturing and installation costs. On the other hand, plate heat exchangers achieve up to 95% thermal efficiency due to their extensive surface area, while compact heat exchangers provide high heat transfer coefficients relative to their small size, as a result of a large heat transfer

area. Both types surpass DPHEXs in thermal performance theory [3, 4].

In most industries today, there is a unified trend toward energy saving, increasing efficiency, and reducing the size and cost of related industrial equipment. Hence, efforts have been made to improve the design of heat exchangers to enhance thermal efficiency and reduce costs and material consumption. Generally, the techniques adopted to boost the heat transfer rate are categorized into two main groups: active and passive [6]. Active methods involve the inclusion of some external energy input to grow heat transfer, through measures such as mechanical additions, the application of a magnetic field to scatter light particles that flow in a specific path, and other similar methods. Conversely, passive methods do not rely on any external energy input. A common approach to improve passive heat transfer performance is by increasing the surface area and thermal residence time between two fluids. This method leads to an increase the turbulence of fluids flow, thus improving the surface area, while maintaining the time and heat transfer coefficient of the current system [7]. Any enhancement in the overall heat transfer coefficient, heat transfer surface area, or temperature difference between the hot and cold fluids in heat transfer systems is imperative to refine heat transfer rates, as indicated by the general equation expressing thermal performance in heat transfer systems  $q = U A_s \Delta T_{LMTD}$ . Initially, the finite volume method (FVM) is a computational numerical technique used in engineering to convert partial differential equations formulating conservation laws over differential volumes into individual algebraic equations on specific or finite volumes. It underpins to conservation quantities like mass and energy, making it extremely fitted for CFD analysis and industrial product development [8]. On the flip side, genetic algorithm (GA) is a common solution method in Evolutionary computation (EC) techniques that consists of various algorithms based on the principle of evolutionary search for optimal solutions to particular problems [9]. GAs have been shown high potential in optimizing heat exchangers through search process and joint optimization of thermal problems [10]. Therefore, GA enhancement of DPHEX study model is performed under the constraint of allowable pressure drop to achieve optimal results according to the specified design objectives. Thus, the literature review related to the project's objectives is summarized, which

regards simulating and enhancing the performance of DPHEXs using ANSYS FLUENT software and GA as follows: Mohsen Amini et al. (2013), developed a methodology to optimize shell-and-tube heat exchangers with the goals of increasing heat transfer rate and reducing total cost. Due to the significant relationships between the objective functions and the variables, eleven variables were scrutinized for improvement using the Genetic Algorithm. Results from two studies demonstrated improvements in both heat transfer rate and cost reduction compared to existing data. The value of this study lies in practical recommendations for heat exchanger design [11]. Kale Shivam B et al. (2017), performed a CFD analysis to assess flow conditions with and without braided tape. The comparison between CFD and experimental results was highly satisfactory. Nusselt number, effectiveness, and heat transfer coefficient were determined and contrasted. The braided tape increased heat transfer rates and exchanger effectiveness. Differences between experimental and CFD results accounted for the following variances: Nusselt number (1–7%), heat transfer coefficient (3–13%), and effectiveness (5–11%). Temperatures from CFD and experimental readings were within reasonable limits [12]. Peddi Dilleswara Rao et al. (2017), considered counterflow and straight tube/U-shaped configurations under specific operating conditions. Turbulence models in CFD simulations were validated by comparing outlet temperature profiles. Results using the K- $\epsilon$  turbulence model in Ansys Fluent were satisfactory. Nusselt number and velocity/pressure distributions were analyzed, emphasizing the importance of selecting an appropriate turbulence model based on experimental data for accurate evaluation of heat exchanger performance [13]. Mohammad Hemmat Esfe et al. (2017), highlighted the enhancement of heat transfer coefficient in MgO-water nanofluids. To derive the heat transfer coefficient and cost functions, experimental data were used via the Response Surface Method, and next applied the non-dominated sorting genetic algorithm for improvement. Demonstrated effectiveness of the approach with a significant reduction in cost, approximately 38% [14]. Baru Debtera et al. (2018), compared actual heat transfer using the number of transfer units (NTU) method and computational fluid dynamics (CFD). Results showed high agreement, with minimal deviation: 29.7 kW from simulation and 30.0 kW NTU method. Hot

fluid entered at 415 K, and cold fluid circulated at 300 K. Simulations provided elaborated insights into heat, hydrodynamics, and fluid velocities, with capturing temperatures of 407.106 K for hot fluid and 306.77 K for cold fluid [15]. Vikas Kanjariya et al. (2018), conducted an analysis evaluated DPHEX performance of under varying flow conditions through experimental testing and CFD simulations. The counterflow configuration overshadowed parallel flow, with 29.4% higher effectiveness at a low flow rate (0.02 kg/s). At a higher flow rate (0.10 kg/s), the effectiveness difference decreased to 6.3%. Heat transfer rate correlated with flow rate, with only a 9.3% increase in counterflow at 0.10 kg/s. Effectiveness inversely related to log mean temperature difference (LMDT) [16]. Shreyas Kotian et al. (2020), presented an analysis comparing experimental and numerical studies of DPHEXs using CAD design and Ansys Fluent simulations. Experiments covered Reynolds numbers (60–240), and temperatures (hot fluid: 50 °C and 70 °C; cold fluid: 31 °C). Results indicated significant thermal property variations with inlet temperatures and Reynolds numbers, with CFD analysis closely matched experimental data, showing a maximum 10% error rate [17]. Chakransh Chourase et al. (2023), focused on developing the thermal performance of the heat exchanger using nanofluids through CFD analysis. Nanofluids of copper oxide (CuO), aluminum oxide (Al<sub>2</sub>O<sub>3</sub>), silicon oxide (SiO<sub>2</sub>), and ethylene glycol were applied at volume fractions of 0.2% to 0.4%. Results showed that increasing volume fractions improve heat exchanger performance by enhancing heat transfer rate and coefficient, with CuO giving the best performance, followed by Al<sub>2</sub>O<sub>3</sub> [18]. Javid Zamani et al. (2023), investigated the effectiveness of phase change materials (PCMs) in a DPHEX system for thermal energy storage. An adiabatic interval was introduced to improve charging and discharging processes, during which the pump power is cut off, and water flow stops. Using GA with goals to maximize the stored energy or minimize exergy destruction, results showed the approach's effectiveness [19].

The aforementioned studies showcased the value of using CFD analysis with ANSYS FLUENT and SOLIDWORKS, combined with GA techniques, for industrial heat transfer applications. The review underscores a strong incentive to employ these methods, particularly as this work pioneers experimental study applications of simulation and CFD analysis to a DPHEX in a

low-density polyethylene (LDPE) Unit. The current study intends to accomplish several procedures, including:

Estimate and foster the overall heat transfer coefficient through CFD analysis by ANSYS FLUENT and applied GA, to upgrade the quality of heat exchange process in DPHEX.

Execute a numerical investigation of DPHEX simulation with ANSYS FLUENT at different mass flow rates to examine optimal operating conditions at the as-built heat exchange. Re-employ these outcomes to earn financial and environmental benefits simultaneously.

Execute a computational investigation of DPHEX with GA at different mass flow rates. This study involves optimizing four key variables: mass flow rate, inner and outer diameters of the pipe side, and inner diameter of the annular side. The estimation of the overall heat transfer coefficient is often related to these variables according to conventional heat exchanger design equations.

## DESCRIPTION OF HEAT EXCHANGER MODEL

The model study employed DPHEX sourced from LDPE unit at a State Company for Petrochemical Industries in Basra, Iraq. The heat exchanger designed to cool ethylene gas (9159 kg/hr) in the pipe-side, reducing its temperature from 91.6 °C to 59 °C at a pressure of 99.1 kg/cm<sup>2</sup>. This cooling process was achieved by flowing cooling water (73860 kg/hr) in the annulus-side, which was heated from 32.2 °C to 36.6 °C at a pressure of 5.5 kg/cm<sup>2</sup>. While a fouling resistance was 0.0002 and 0.00041 for the water stream and ethylene stream, respectively. The dimensions of DPHEX model, as physically constructed for the LDPE unit, are presented in Table 1.

## DESCRIPTION DESIGN CALCULATION EQUATIONS

The classical procedure for designing DPHEX model involves several key steps based on energy and material balances as well as the application of heat transfer equations. Certain assumptions are made during the design process, such as steady-state heat balance, absence of heat seepage, no viscous dissipation, no heat generation, a counter-flow configuration for DPHEX, and no phase change. The

**Table 1.** Geometrical parameters of DPHEX

The inner pipe inside diameter, mm	59.00
The inner pipe outside diameter, mm	73.02
The outer pipe inside diameter, mm	128.19
The outer pipe outside diameter, mm	141.30
The exchanger length, mm	6000
The height of outer pipe, mm	420
The pipes material	Steel

design task entails calculating the common key variables, including heat duty (q, W), heat transfer area (A, m<sup>2</sup>), heat capacity rates (C, W/K), overall heat transfer coefficient (U, W/m<sup>2</sup>. °C), and heat transfer efficiency. The design procedure typically follows these steps [20, 21]:

- Estimation of mass velocity

$$G_i = \frac{4 m'_h}{\pi D_i^2} \quad (1)$$

$$G_o = \frac{4 m'_c}{\pi (d_o^2 - d_i^2)} \quad (2)$$

- Estimation of Reynolds number is built upon the stream flow conditions

$$Re_i = \frac{4 m'_h}{\pi d_i \mu_h} \quad (3)$$

$$Re_o = \frac{4 m'_c}{\pi (D_i - d_o) \mu_c} \quad (4)$$

- Estimation of Prandtl number

$$Pr_i = \frac{\mu_h Cp_h}{k_h} \quad (5)$$

$$Pr_o = \frac{\mu_c Cp_c}{k_c} \quad (6)$$

- Estimation of the Nusselt number using Dittus-Boelter correlation equation

$$Nu_i = 0.023 Re_i^{0.8} Pr_i^{0.3} \quad (7)$$

$$Nu_o = 0.023 Re_o^{0.8} Pr_o^{0.3} \quad (8)$$

- Estimation of heat transfer coefficient for turbulent flow in the region (DG/μ >10000) is outlined by Sieder and Tate

$$h_i = 0.023 \frac{k_h}{d_i} \left( \frac{d_i G_i}{\mu_h} \right)^{0.8} \left( \frac{Cp_h \mu_h}{k_h} \right)^{1/3} \left( \frac{\mu_h}{\mu_w} \right)^{0.14} \quad (9)$$

$$h_o = 0.023 \frac{k_c}{De} \left( \frac{De G_o}{\mu_c} \right)^{0.8} \left( \frac{Cp_c \mu_c}{k_c} \right)^{1/3} \left( \frac{\mu_c}{\mu_w} \right)^{0.14} \quad (10)$$

$$De = \frac{D_i^2 - d_o^2}{d_o} \quad (11)$$

- Estimation of temperature at wall surface is essential for determining the viscosity at that location

$$T_w = \frac{(h_i T_{av,i}) + (h_o T_{av,o} D_{ratio})}{h_i + h_o D_{ratio}} \quad (12)$$

- Estimation of the total resistance posed by both the tube wall and any accumulated dirt factors

$$R_{dw} = \frac{d_o(d_o - d_i)}{k_w D_{lm}} + \frac{d_o}{d_i h_{di}} + \frac{1}{h_{do}} \quad (13)$$

- Estimation of heat exchanger parameters effectiveness

$$U_c = \frac{h_i h_o}{h_i + h_o} \quad (14)$$

$$U_d = \frac{1}{\frac{1}{U_c} + R_{dw}} \quad (15)$$

$$q = \dot{m}_h C p_h (T_{hi} - T_{ho}) = \dot{m}_c C p_c (T_{co} - T_{ci}) = U_o A_o \Delta T_{lm} \quad (16)$$

$$\Delta T_{lm} = \frac{(T_{ho} - T_{ci}) - (T_{hi} - T_{co})}{\ln \left( \frac{T_{ho} - T_{ci}}{T_{hi} - T_{co}} \right)} \quad (17)$$

$$A_o = \frac{q}{U_d \Delta T_{lm}} \quad (18)$$

- Estimation of tube side pressure drop

$$f_i = \frac{0.04}{\left( \frac{d_i G_i}{\mu_h} \right)^{0.16}} \quad (19)$$

$$\Delta P_i = \frac{2 f_i G_i^2 L}{\rho_i d_o} \quad (20)$$

- Estimation of annular side pressure drop

$$f_o = \frac{0.04}{\left( \frac{(D_i - d_o) G_o}{\mu_c} \right)^{0.16}} \quad (21)$$

$$\Delta P_o = \frac{2 f_o G_o^2 L}{\rho_o (D_i - d_o)} \quad (22)$$

- Estimation of heat exchanger efficiency

$$\epsilon = \frac{1 - \exp[-(UA/C_{min}) (1 + C_{min}/C_{max})]}{1 + C_{min}/C_{max}} \quad (23)$$

where:  $T_{hi}$  – temperature of the hot fluid entrance on the pipe-side (°C);  $T_{ho}$  – temperature of the hot fluid exit on the pipe-side (°C);  $T_{ci}$  – temperature of the cold fluid entrance on the annulus-side (°C);  $T_{co}$  – temperature of the cold fluid exit on the annulus-side (°C);  $T_{av, i}$  – average temperature on the pipe-side (°C);  $T_{av, o}$  – average temperature on the annulus-side (°C);  $\Delta T_{lm}$  – global mean temperature difference (°C);  $U_c$  – clean overall heat transfer coefficient (W/m<sup>2</sup>, K);  $U_d$  – dirty overall heat transfer coefficient (W/m<sup>2</sup>, K);  $A_o$  – outside heat transfer area (m<sup>2</sup>);  $A_i$  – inside heat transfer area (m<sup>2</sup>);  $D_i$  – inside diameter of the outer pipe (m);  $d_o$  – outside diameter of the inner pipe (m);  $d_i$  – inside diameter of the inner pipe (m);  $D_{lm}$  – log mean diameter (m);  $f$  – the friction factor;  $G_i$  – pipe-side mass velocity (kg/m<sup>2</sup>s);  $G_o$  – annulus-side mass velocity (kg/m<sup>2</sup>s);  $\dot{m}_c$  – mass flow rate of cold fluid (kg/hr);  $\dot{m}_h$  – mass flow rate of hot fluid (kg/hr);  $L$  – length of the heat exchanger tube (m);  $k_h$  – Thermal conductivity of ethylene gas at bulk temperature (W/m·K);  $k_c$  – thermal conductivity of cooling water at bulk temperature (W/m·K);  $k_w$  – thermal conductivity of steel wall

(W/m·K);  $\mu_h$  – viscosity of ethylene gas at bulk temperature (Pa·s);  $\mu_c$  – viscosity of cooling water at bulk temperature (Pa·s);  $\mu_w$  – viscosity at wall temperature (Pa·s);  $Cp$  – specific heat at average bulk temperature of fluid (J/kg·K).

## WORK METHODOLOGY

This work involved conducting a study to assess the heat exchanger’s performance, which occurred in two stages: enhancing the design parameters including pipe diameters, length, heat exchange surface area, and optimizing operational conditions such as fluid velocity, temperature, and pressure drop. These combined conditions ultimately resulted in elevating the overall heat transfer coefficient.

### Description genetic algorithm toolbox of matlab application

This project direction is towards of utilizing Microsoft’s Component Object Model (COM) server to generate a special interface between Aspen Hysys® with MATLAB’s GA toolbox. The primary objective of hiring Aspen Hysys® is to consistently acquire the physical properties of ethylene gas and cooling water across varying operating conditions throughout the solution search phase with GA. In this study, the algorithm was employed to optimize four decision variables: mass flow rate of cooling water x(1), inside diameter of inner pipe x(2), outside diameter of inner pipe x(3), and inside diameter of outer pipe x(4), aiming to increase the objective function, which is the overall heat transfer coefficient. The algorithm embarks on a search journey to find the obvious optimal solution by evaluating all potential solutions within the population. Initially, the objective function is computed to form the initial population, and a subset of warrior chromosomes is selected based on superior performance. These chromosomes undergo crossover and mutation processes to generate diverse offspring. Crossover merges genetic material from the selected champion chromosomes and transferring genes from older chromosomes to the new generation, while mutation introduces novel genetic variations. The process, including selection, crossover, mutation, and replacement, repeats in a continuous loop based on a unified solution map. Throughout the replication stages, following the principle of survival of the fittest, the strongest chromosomes replace

weaker ones until a stopping criterion, determined by the penalty function, is met [9]. Conventional criterion involve constraints on the inner and outer diameters of the tube side and a maximum allowable pressure drop, as indicated in several studies [22]. In this work, artificial penalty terms were enforced for significant constraint violations, specifically when  $x(3) < x(2)$ ,  $x(3) - x(2) < 0.0005$ , and if the pressure drop exceeded 70000 Pa. The solution space is constrained within specific ranges:  $x(1)$  ranges from 50000 to 90000 kg/hr,  $x(2)$  varies from 0.03 to 0.12 m,  $x(3)$  ranges from 0.06 to 0.13 m, and  $x(4)$  spans from 0.1 to 0.15 m. It's worth noting that these dimensions are committed to the acceptable standards set by TEMA. The settings for GA toolbox are as follows: the population size is set to 50 individuals, the number of generations is limited to 100, the selection method employed is tournament selection with a tournament size of 4, both crossover and mutation operators are constraint dependent, and the stopping criterion is defined as  $10^{-6}$ . The optimization procedure steps with GA for the DPHEX, as shown in Figure 2, embedded the design equations defined in the previous section.

### Description design with CFD ANSYS FLUENT

The simulation process in CFD entails several steps, including geometry creation (which is facilitated within SOLIDWORKS software in this study), mesh generation, selection of appropriate models and boundary conditions, solving the equations numerically, and post-processing the results by employing CFD simulations, the analysis of fluid flow within DPHEX using ANSYS FLUENT software can encompass multiple aspects of the investigation study, including the examination of flow velocities and pressure distributions, heat transfer rates, and other relevant properties. CFD provides a crucial view for the prediction and visualization of fluid behavior under varying operating conditions and geometries.

### Geometric modeling for heat exchanger

The three-dimensional model of DPHEX, as shown in Table 1, with six pipes, was built via SOLIDWORKS software, as depicted in Figure 3. SOLIDWORKS proves a striking role in the design and simulation process, providing an

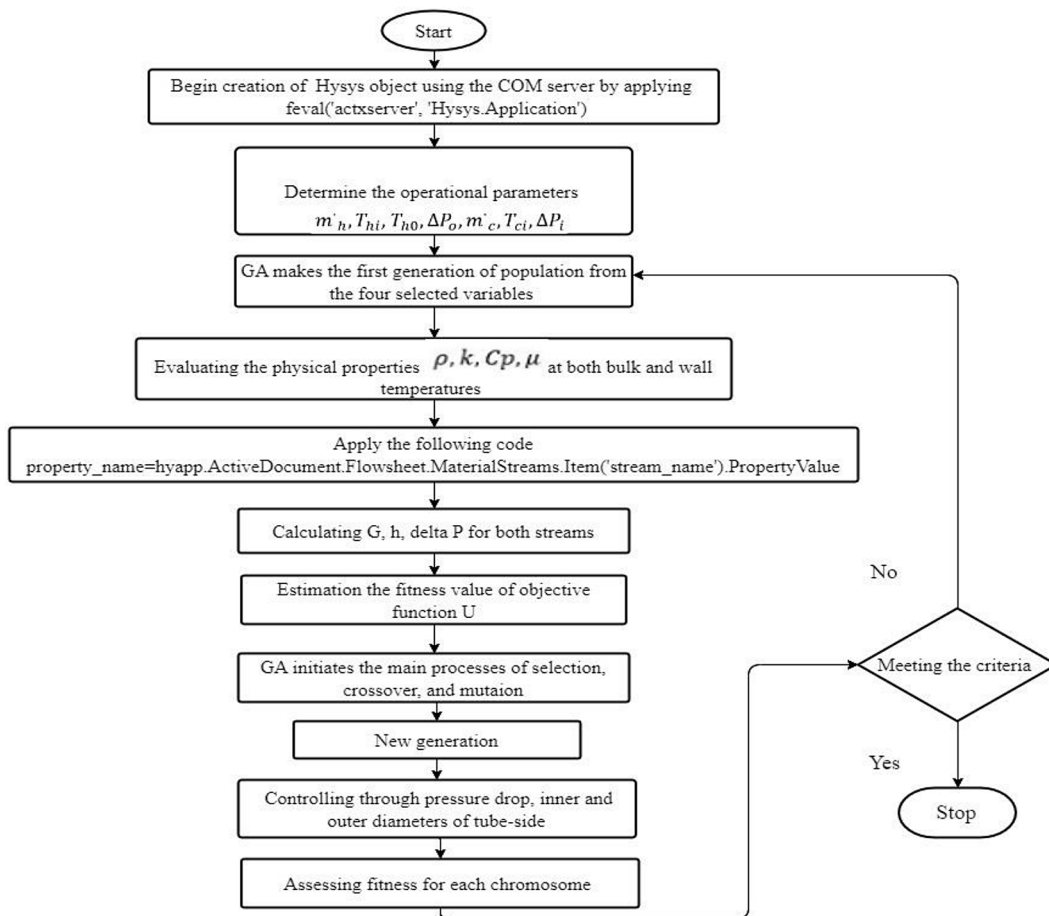


Figure 2. Flowchart steps to optimize overall heat transfer coefficient of DPHEX with GA

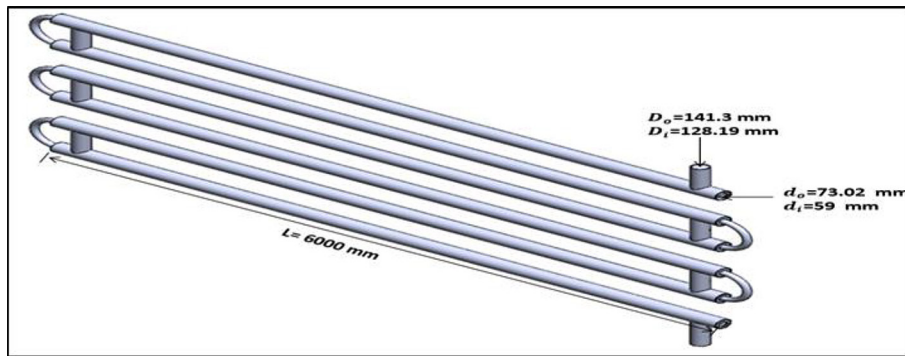


Figure 3. Geometry construction of a DPHEX with SOLIDWORK

extensive engineering environment with advantages such as a user-friendly interface, efficient drawing capabilities, ease of design modification, and the ability to simulate complex physical systems. Features such as extruded boss/base, extruded cut, swept cut, extruded surface, and knit surface, which contributed to creating the exchanger geometry with meticulous details, precision, and efficiency.

*Meshed geometry*

The DPHEX geometry was meshed using ANSYS FLUENT v. 2022 R1. The meshing procedure entailed subdividing the geometry into smaller elements, which is essential for the numerical solution of mathematical equations at each element’s center. This approach enabled ANSYS FLUENT to provide results across the entire domain of DPHEX by interpolating the values from each element center. To assess the influence of mesh on the simulation results, a grid test was implemented to evaluate the overall heat transfer coefficient using 2812233 to

7030583 elements, as presented in Figure 4, which varied from 666 to 676.8 W/m<sup>2</sup>·K with 1.5% error. In this study, the mesh selected was configured as follows: A uniform mesh size of 4.5 mm was applied to six exchanger pipes, yielding a total of around 4,218.350 elements and 2,189.214 nodes. Tetrahedral cells were chosen for the pipe and annulus bodies, for their superior capability to capture curvatures accurately. This method was selected to guarantee a more precise portrayal of the complex geometry. To enhance the mesh quality on the walls, inflation layers were added (5 layers, 0.3–1.2 mm thick), as shown in Figure 5a, b. Ensuring the integrity and quality of mesh is paramount for tuning the stability of the numerical computation and attaining reliable simulation outcomes. Various criteria, including aspect ratio, skewness, and orthogonality, to evaluate the health of mesh. The acceptable range for these mesh metrics is as follows: an aspect ratio falling between 1 and 10 [23], a skewness greater than 0 and less than 0.9, with values closer to 0 deemed

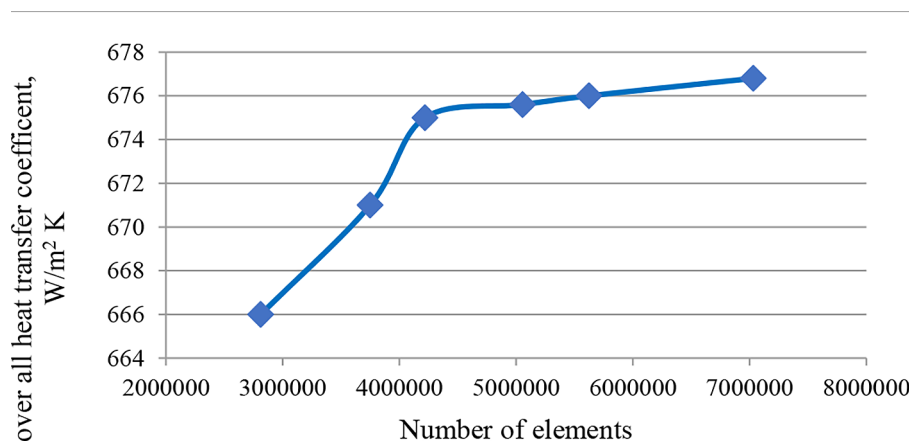
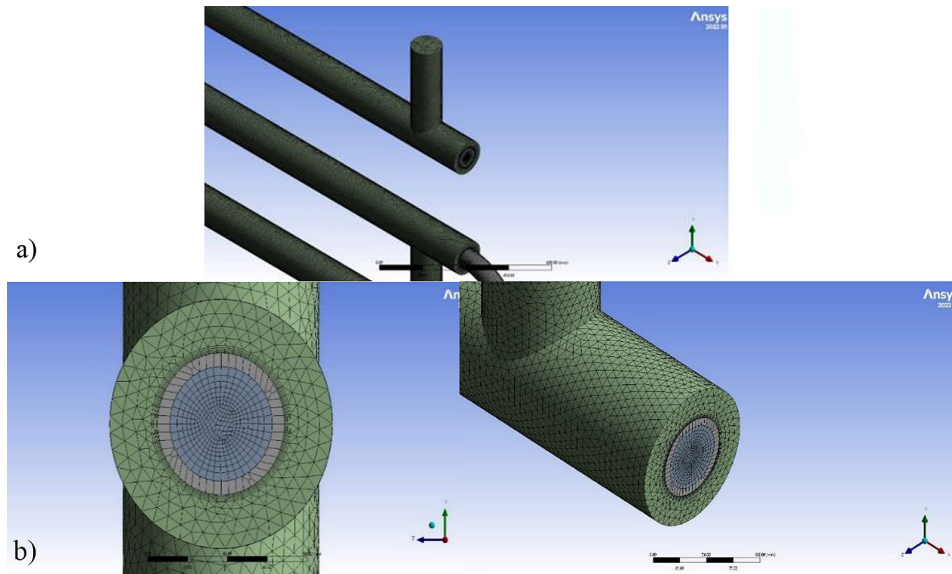


Figure 4. Mesh independence study on overall heat transfer coefficient at various number of elements



**Figure 5.** a) Grid system of DPHEX, b) Inlet region scheme achieved after implementing the appropriate size, method, and inflation techniques

preferable, orthogonality between 0.7 and 0.9, with values closer to 1.0 preferred, and an element quality of 0.8 or higher is considered satisfactory [24]. In this study, achieving good convergence within these specified ranges for these metrics was pursued with dependable results, as indicated in Table 2. Figures 6 to 8 showed the values of metrics which are represented by the x-axis, and the y-axis represents the number of elements. Selecting any bar displays the locations of these elements in the mesh. All metrics were within the valid ranges that promote the adoption of generated mesh.

### Boundary conditions

To complete the solution setups for this particular configuration applied a set of assumptions: Firstly, the flow is considered steady-state and incompressible. Secondly, the outer surface of the annulus pipes is assumed to be adiabatic, while the fluid within the pipes is regarded as a single-phase exhibiting turbulent flow. Moreover, a constant mass flow rate is maintained for ethylene gas, the hot fluid within the inner pipe, while cooling water circulates through the outer pipe. Boundary conditions are enforced on both the pipe and annulus sides.

**Table 2.** Mesh metrics of DPHEX generation

Geometry	Average skewness	Average orthogonal quality	Average aspect ratio	Average element quality
Pipe and annulus	0.1895	0.83043	6.7978	0.8720

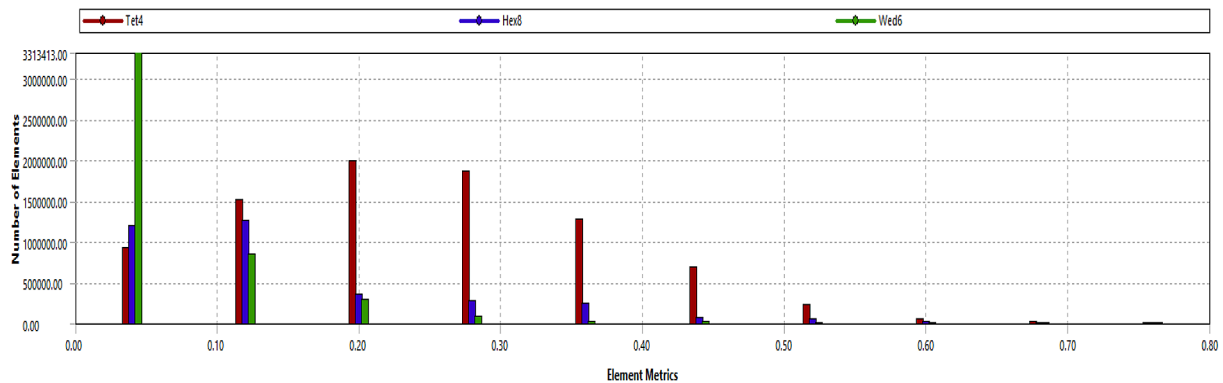


**Figure 6.** Quality of skewness in the mesh elements



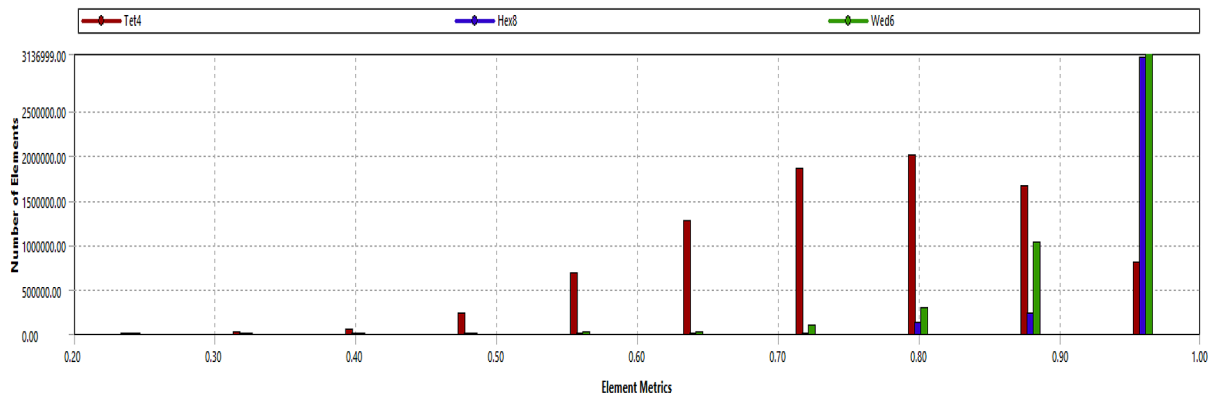


Figure 7. Quality of orthogonal in the mesh elements

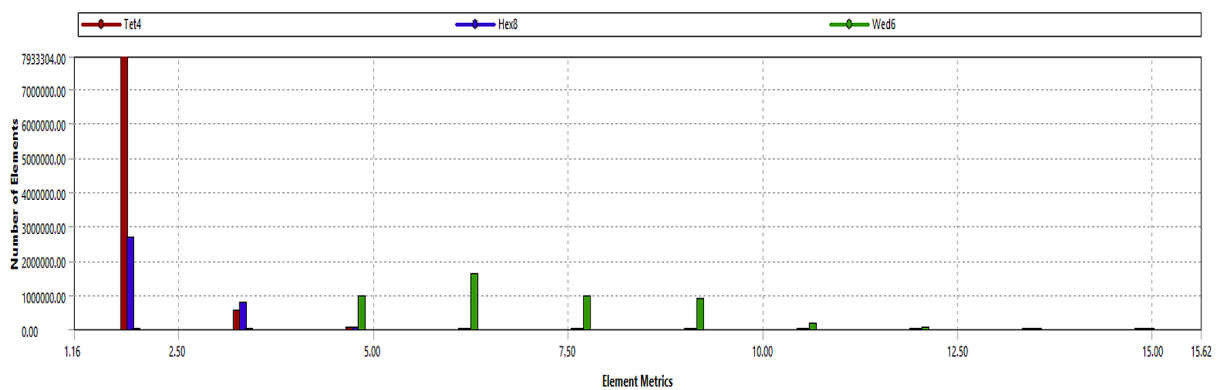


Figure 8. Quality of aspect ratio in the mesh elements

Since the flow occurs vertically in multiple pipes, the impact of gravity is factored in, considering a gravitational acceleration of  $-9.810\text{m/s}^2$  along the y-axis. The application of the  $k-\epsilon$  model is adopted to accommodate turbulent flow and heat transfer phenomena. The inlet conditions for both the cooling water and ethylene gas are specified by their mass flow rates and temperatures. outflow conditions are set as pressure outlets ( $p_{\text{water}} = 499452.68 \text{ Pa}$ ,  $p_{\text{ethylene}} = 9693873.52 \text{ Pa}$ ) Various flow rates for the cooling water are investigated, spanning from 36000 kg/h to 82800 kg/hr. Regarding the wall conditions, the walls are assumed to be stationary and have no-slip boundary conditions. To address heat transfer, a convection layer with a thickness of 0.0138 m is applied to the inner-pipe walls. Convergence criterion for the solution is determined using a tolerance error value of  $10^{-4}$ , and the solution initialization employs standard computations across all zones.

## RESULTS AND DISCUSSION

In essence work, numerical computations were conducted to investigate DPHEX and to

delved into the mechanism research for determining the optimum heat transfer coefficient solution through a genetic algorithm applied seamlessly to the design calculation equations. To validate the obtained results of ANSYS FLUENT, a useful strategy is to assess the dimensionless number Y-plus, which can be observed and measured exclusively on the walls. This parameter serves as a safe indicator of the fineness of mesh design on the walls. It is considered sensible when the Y-plus value falls within the range of 1 to 60 [25]. The results for the Y-plus values are presented in Table 3, allowing for an evaluation of the mesh quality and its impact on the accuracy of the simulations. Initially, the cooling water mass flow rate used in the analysis was 73.860 kg/hr. The heat transfer phenomena within the model were

Table 3. Average of dimensionless number Y-plus

Average of facet values wall Y-plus	
convection_inner_pipe_wall	32.967312
inner_pipe_wall	28.765767
Net	29.331526

analyzed using ANSYS FLUENT, and the corresponding results are presented in Figure 9a and 9b. It was observed from the temperature distribution map on both the tube and shell sides that the heat transfer was moderated. Some inlet areas of the cooling water indicated poor heat transfer due to the thermal boundary layer still forming in this region. In this case, the heat transfer rate in the modified configuration model via ANSYS FLUENT and GA were 367,020.93 W and 380,755.33 W, respectively, outweighing the original model configuration's 295,721.27 W. Table 4 exhibits the present and simulation model's operational, design, and thermal conditions. Increasing the heat transfer rate in most heat exchangers depends on three primary factors: total heat transfer coefficient, heat transfer surface area, or LMTD. The most appropriate approach involved increasing the total heat transfer coefficient. The discrepancy between the results of the two optimization procedures can be attributed to the focus in the GA solution's on advancing

the objective function, U, within specific constraints. This leads to distinctions in the outlet temperatures of cooling water when employing ANSYS FLUENT and GA, which were 34.5 °C and 37.29 °C, in that order.

Figure 10a and 10b illustrates the velocity distribution among the shell and tube sides, highlighting the role of fluid movement in the convection heat transfer mechanism. Furthermore of thermal conduction, heat transfer relies on the fluid's motion within the pipes. ANSYS reveals that the heat transfer between two fluids is enhanced as the fluid velocity rises. For the tube side, the velocity ranges from 1.65 to 1.74 m/s, while on the shell side, it ranges from 3.21 to 3.26 m/s. Notably, this increased velocity further contributes to a higher heat transfer rate. It is worth noting that the velocity and temperature of the cooling water leaving this exchanger, present model, were 1.22 m/s and 36.6 °C respectively, while the results of ANSYS FLUENT simulation were 1.7m/s and 34.5 °C. This supports the constructed simulation,

**Table 4.** Simulation and optimization results of DPHEX

Parameters	Tube-side values			Shell-side values		
	Present model	Numerical solution	Optimum solution - GA	Present model	Numerical solution	Optimum solution - GA
Entering temperature, °C	91.6	91.6	91.6	32.2	32.2	32.2
Leaving temperature, °C	59	49.45	50	36.6	34.5	37.29
Flow rate, kg/hr	9159	9159	9159	73860	73860	59233.45
Pressure drop, Pa	24516.60	–	15170.52	39913.06	–	55769.53
Heat transfer rate, W	Present model		Numerical solution		Optimum solution - GA	
	295721.27		367020.93		380755.33	
overall tubes length, m	36		36		60	
Total surface area, m <sup>2</sup>	17		17		21.12	
LMTD, °C	39		33.9		32.73	
Objective function: Overall heat transfer coefficient, W/m <sup>2</sup> ·K	440		675		751	

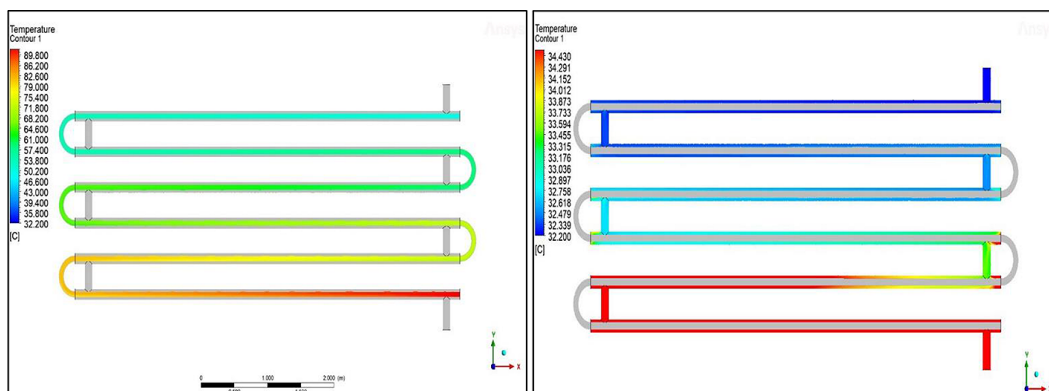


**Figure 9** a) Temperature distribution of tube-side DPHEX, b) Temperature distribution of shell-side DPHEX

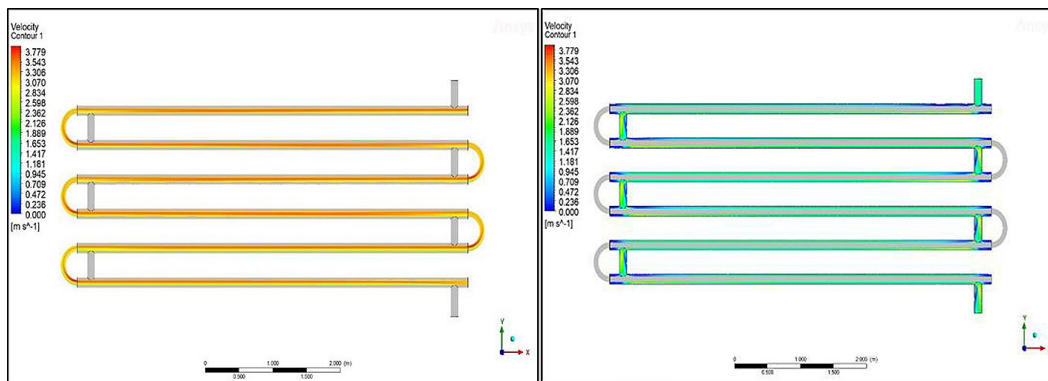


Figure 10. a) Velocity contour of tube-side DPHEX, b) Velocity contour of shell-side DPHEX

as the fluid temperature is inversely proportional to the flow velocity. Figure 11 shows how the outlet temperature of gas ethylene changes moderately with varying inlet velocities of the cooling water flowing from 0.80 to 1.85 m/s.

Another significant factor affecting thermal performance is the pressure drop (PD), through represents a vital role in determining the pumping power and, consequently, the operating cost of the heat exchanger. The forerunner objective was to balance increasing the total heat transfer coefficient while minimizing PD. According to the results from GA, increasing the pipe-side inner diameter by 19%, the outer diameter by 22%, and reducing the fluid velocity to 2.17 m/s collectively contributed to a lessening in PD. Meanwhile, decreasing the inner diameter on the annulus-side and raising the fluid velocity to 3.6 m/s caused a rise in PD within sensible limits. Additionally, extending the tube length increased the tube surface heat exchange area, thereby augmenting the convection heat transfer coefficient. The values of the decision variables obtained from the optimization algorithm for DPHEX were as follows:  $x(1) = 59233.45$  kg/h,  $x(2) = 0.0730$  m,  $x(3) = 0.0936$  m, and  $x(4) = 0.1274$

m. It can be seen from Figure 12 the relationship between the mass flow rate and the overall heat transfer coefficient. Thermal calculations were performed to periodically assess the overall heat transfer coefficient at various flow rates of cooling water. Concurrently, suitable operating conditions and variables were selected that optimize the heat transfer process, while declining water consumption, thus promoting saving-energy and environmental responsibility. The graph presents a clear upward trend of the ANSYS FLUENT and GA series, indicating that as the flow rate increased, the total heat transfer coefficient also grew. This relationship is attributed to the rise in the temperature difference between the hot and cold fluids, resulting in a greater amount of heat transfer. Consequently, there is a swelling in heat exchange and the overall heat transfer rate between the water and ethylene gas. The study recorded the highest heat transfer coefficient at approximately  $675 \text{ W/m}^2\cdot\text{K}$  and  $751 \text{ W/m}^2\cdot\text{K}$  of ANSYS FLUENT and GA, respectively, at a flow rate of 20.52 kg/s. The percentage error between the two procedures was approximately 11%. The function of CFD analysis provided the numerical

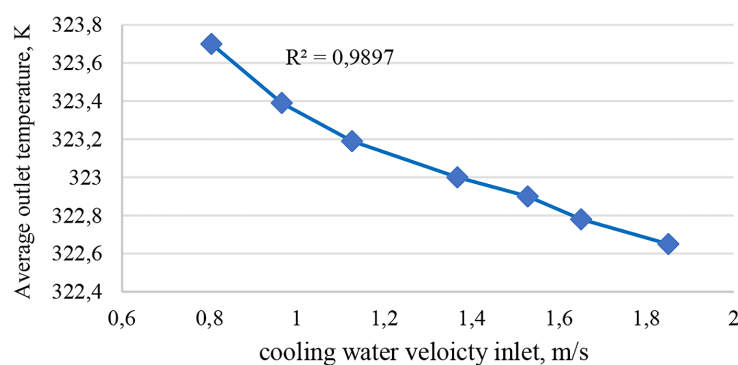


Figure 11. Temperature vs. velocity

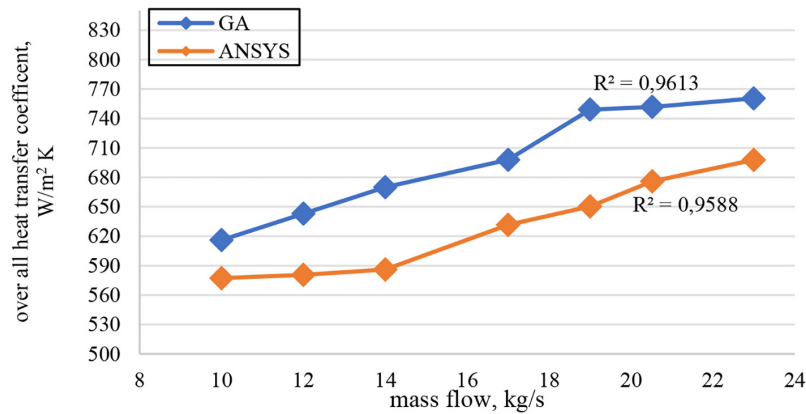


Figure 12. Overall heat transfer coefficient against mass flow rate

solution to the heat transfer problem, while GA sought to obtain the optimization solution.

Figure 13 depicts the convergence curve of the exhaustive optimization algorithm to increase overall heat transfer coefficient. The best value of objective function is plotted for each generated iteration. The optimal value is reached after 89 iterations of the algorithm. In addition to, Figure 14 shows the scores of each individual generated, where the majority of individuals scored between 700 and 750, which accounts for the stability marked in the convergence curve due to the high concentration of scores in this column.

The logarithmic mean temperature difference (LMTD) is an essential concept in heat transfer systems as it helps determine the driving force, much like an engine, for heat exchange process.

In the present study, LMTD was calculated using ANSYS FLUENT at various mass flow rates of water. The results show a clear direction of growing LMTD with an increase in mass flow rates, as illustrated in Figure 15. This positive relationship confirms that increasing temperature difference between the fluids improves the efficiency of heat transfer through the exchanger, a higher LMTD enhances overall heat transfer coefficient in DPHE.

The relationship between Reynolds number and Nusselt number is complex and dependent on several factors such as flow type, geometry design, and the heat transfer mechanism involved. Generally, a higher Reynolds number leads to more turbulent flow, which enhances convective heat transfer by creating eddies and increasing

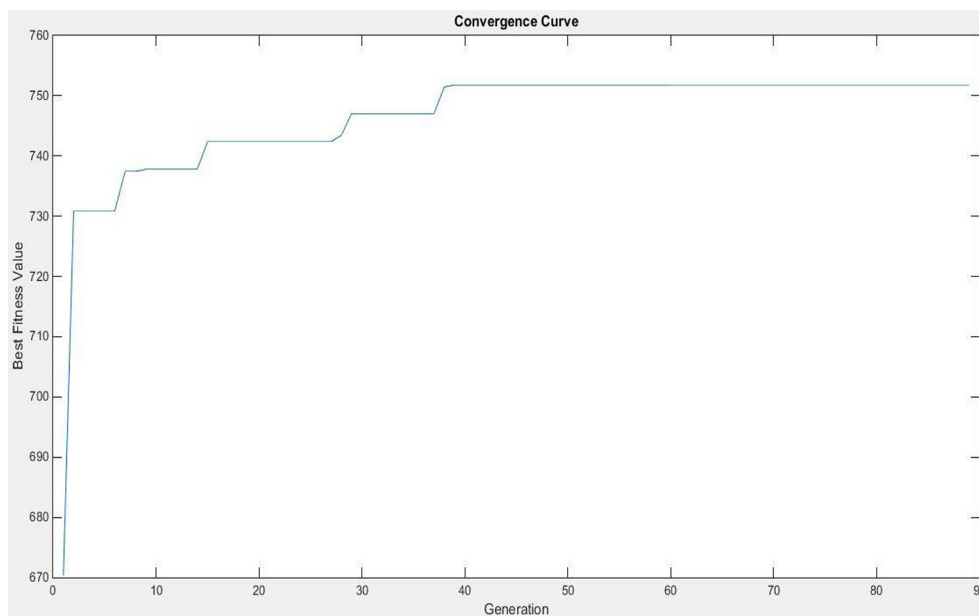


Figure 13. Best fitness value at each generation

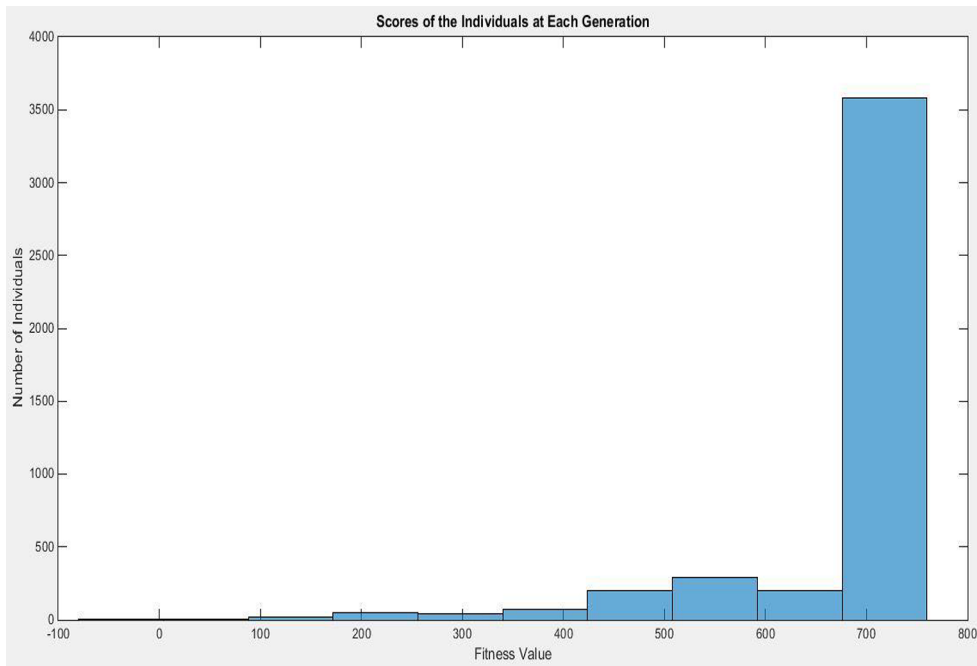


Figure 14. Fitness value of the individuals at each generation

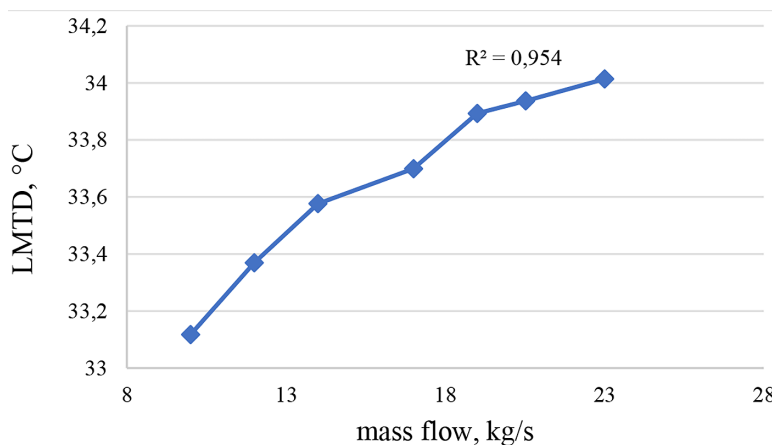


Figure 15. LMTD against mass flow rate

fluid motion. Consequently, the heat transfer rate increases, and Nusselt number, which represents the efficiency of heat transfer, also tends to rise. However, due to the intricate nature of heat transfer phenomena, the specific relationship between Reynolds number and Nusselt number often requires empirical correlations or detailed analysis based on experimental data and numerical simulations. In this work, GA procedure evaluates Re and NU under the critical assumption that factors such as pipe-side and annular side diameters, viscosity, and mass flow rate change, to accurately determine and predict heat transfer characteristics. Figure 16 indicated that the relationship is

direct, with the Reynolds number reaching a value of 724179.64 and the Nusselt number attaining 1809.08 at a cooling water flow rate of 20.52 kg/s.

For Figure 17, in general, increasing the mass flow rate typically makes heat transfer more efficient. More fluid passes through the heat exchanger per unit time when the mass flow rate is raised. At a flow rate of 20.52 kg/s, the heat exchanger achieved its highest effectiveness of up to 87.7% and 88.6% as determined by ANSYS FLUENT and GA, respectively, providing exceptional thermal performance. However, when the flow rate was reduced to 14 kg/s, the effectiveness of heat exchanger went down to around 82%.

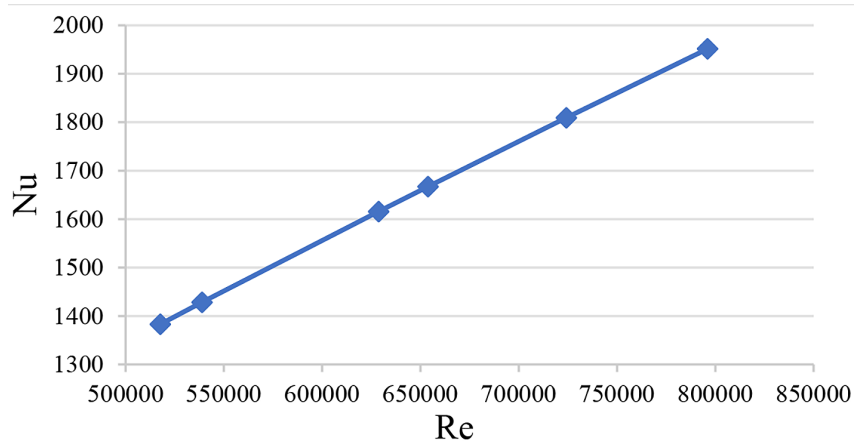


Figure 16. Nusselt number against Reynold’s number

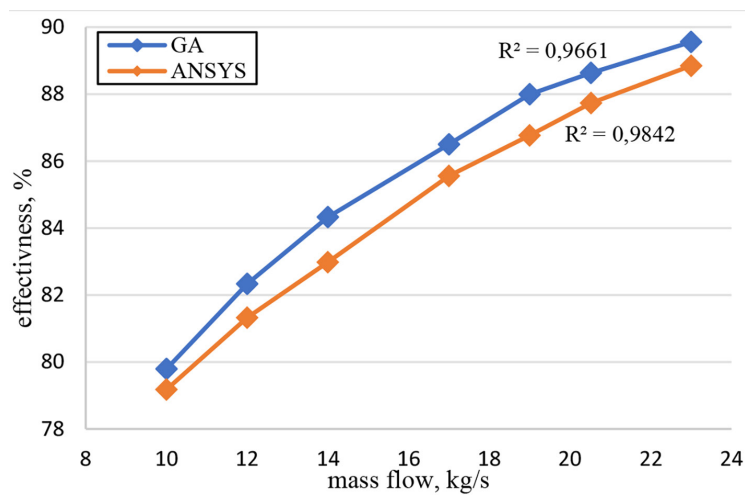


Figure 17. Mass flow rate versus effectiveness

## CONCLUSIONS

In the present work, the heat transfer characteristics of DPHEX were studied through a computational investigation to determine the optimum design and operating parameters. The carefully constructed mesh in ANSYS FLUENT, combined with GA, provided a solid foundation for conducting simulations and acquiring rigorous results for the six-pass DPHEX. The main results obtained can be outlined as follows:

The temperatures of entry and exit of ethylene gas flowed in the inner pipe were 364.6 K (91.6 °C) and 322.6 K (49.45 °C), respectively.

The thermal performance of the heat exchanger was analyzed and compared using the two techniques against its actual performance. It was observed that the optimum heat transfer rate reached 367 KW with ANSYS FLUENT and 380 KW with GA, revealing an important increase of

roughly 24% and 28%, respectively, compared to the original model value. This results was achieved with the assistance of multiple factors, the most efficient being the improvement of the heat transfer coefficient, which is associated with increased fluid velocities and optimized geometric features of DPHEX.

The potential of genetic algorithm was evident in enhancing the overall heat transfer coefficient of DPHEX. Through dedicated research across a wide solution space and under various operating conditions of DPHEX, the results of the four decision variables were sent to Aspen HYSYS® software to capture material properties aligned with the operating specifications and generate a new solution at each iteration.

The DPHEX effectiveness was estimated to be around 87% to 88%. These findings indicate that the heat exchanger performed well and demonstrated high thermal efficiency, confirming the soundness

of strategy. Under these circumstances, there is a distinct opportunity to attain higher performance efficiency by integration the optimized geometry of DPHEX proposed by GA with CFD analysis.

Another direction was implemented in an experimental study with varying cooling water flow rates at different levels: 36000 kg/h, 43200 kg/h, 50400 kg/h, 61200 kg/h, 68400 kg/h, 73860 kg/h, and 82800 kg/h. The results indicated that it was possible to minimize the mass flow rate of water by 46% compared to the initial flow rate. Despite the reduction in flow rate, the heat exchanger still maintained an acceptable effective performance, with a heat transfer rate of 361 KW.

Simulation and modeling studies of heat exchangers have a powerful and influential role, making them extremely applicable for use in various industrial sectors. These studies display worthy information about how heat exchangers perform in various environments, empowering engineers and researchers to improve designs, enhance energy efficiency, and save costs.

### Acknowledgements

We are thankful to the State Company for Petrochemical Industries in Basra, Iraq. Particularly, Low-Density Polyethylene unit members, to back up this work with design and operating data of DPHEX that served at this unit.

### REFERENCES

1. Mahdi MS, Mahood HB, Hasan AF, Khadom AA, Campbell AN. Numerical study on the effect of the location of the phase change material in a concentric double pipe latent heat thermal energy storage unit. *Thermal Science and Engineering Progress*. 2019; 11: 40–49.
2. Molana M. A Comprehensive review on the nanofluids application in the tubular heat exchangers. *American Journal of Heat and Mass Transfer*. 2016; 3(5): 352–381.
3. Edreis E, Petrov A. Types of heat exchangers in industry, their advantages and disadvantages, and the study of their parameters. In: *Proc. IOP Conf. Series: Materials Science and Engineering 2020*, 963.
4. Pachauri R, Chaturvedi A. Performance Analysis of Compact Heat Exchanger. *International Journal Of Scientific Progress And Research (IJSPR)*. 2018; 54(1): 29–32.
5. Double pipe heat exchangers. S. S. Engineering. Available from: <https://www.ssengindia.com/double-pipe-heat.html>
6. Kola PVKV, Pisipaty SK, Mendu SS, Ghosh R. Optimization of performance parameters of a double pipe heat exchanger with cut twisted tapes using CFD and RSM. *Chemical Engineering and Processing - Process Intensification*. 2021; 163: 108362.
7. Kanojiya NC, Kriplani VM, Walke PV. Heat transfer enhancement in heat exchangers with inserts: a review. *International Journal of Engineering Research & Technology (IJERT)*. 2014; 3(10): 494–500.
8. Moukalled F, Mangani L, Darwish M. *The finite volume method in computational fluid dynamics: an advanced introduction with Openfoam® and MATLAB®*. New York: Springer; 2015.
9. Sivanandam SN, Deepa SN. *Introduction to genetic algorithms*. New York: Springer; 2007.
10. Xie GN, Sunden B, Wang QW. Optimization of compact heat exchangers by a genetic algorithm. *Applied Thermal Engineering*. 2008; 28(8–9): 895–906.
11. Amini M, Bazargan M. Two objective optimization in shell-and-tube heat exchangers using genetic algorithm. *Applied Thermal Engineering*. 2014; 69(1–2): 278–285.
12. Balu KS, Pruthviraj KP, Ganeshsingh PR, C. KS. Experimental analysis & simulation of double pipe heat exchanger. *International Journal of Advance Research and Innovative Ideas in Education (IJARIIE)*. 2017; 3(2): 2357–2367.
13. Rao PD, Rao BN. CFD simulations and validation through test data of a double pipe counter flow heat exchanger. *International Journal of Mechanical Engineering and Technology (IJMET)*. 2017; 8(5): 818–831.
14. Esfe MH, Hajmohammad H, Toghraie D, Hadi Roshtamian, Mahian O, Wongwises S. Multi-objective optimization of nanofluid flow in double tube heat exchangers for applications in Energy Systems. *Energy*. 2017; 137: 160–171.
15. Debtera B, Neme I, S\* VP. CFD Simulation of a double pipe heat exchanger: analysis conduction and convection heat transfer. *International Journal of Scientific Research and Review*. 2018; 7(12): 329–338.
16. Kanojiya V, Gaur R, Yadav P, Sharma R. Performance investigation of a double pipe heat exchanger under different flow configuration by using experimental and computational technique. *Archive of Mechanical Engineering*. 2018; Lxv (1): 28–41.
17. Kotian S, Methekar N, Jain N, Naik P. Heat transfer and fluid flow in a double pipe heat exchanger, part i: experimental investigation. *Asian Review of Mechanical Engineering*. 2020; 9(2): 7–15.
18. Chourase C, Rajpoot SS. Thermal performance and characteristics of double pipe heat exchanger with different nano fluids by using CFD. *International Journal of Research Publication and Reviews*. 2023;

- 4(8): 257–263.
19. Zamani J, Keshavarz A. Genetic algorithm optimization for double pipe heat exchanger PCM storage system during charging and discharging processes. *International Communications in Heat and Mass Transfer*. 2023; 146: 106904.
  20. Peters MS, Timmerhaus KD. *Plant design and economics for chemical engineers*. New York: McGraw-Hill, Inc; 1991.
  21. Çengel YA, Ghajar AJ. *Heat and mass transfer: fundamentals & applications*, fifth edition. New York: McGraw-Hill, Inc; 2015.
  22. Ponce-Ortega JM, Serna-González M, Jiménez-Gutiérrez A. Use of genetic algorithms for the optimal design of shell-and-tube heat exchangers. *Applied Thermal Engineering*. 2009; 29(2–3): 203–209.
  23. Burkhart TA, Andrews DM, Dunning CE. Finite element modeling mesh quality, energy balance and validation methods: A review with recommendations associated with the modeling of bone tissue. *Journal of Biomechanics*. 2013; 46(9): 1477–1488.
  24. Fatchurrohman N, Chia ST. Performance of hybrid nano-micro reinforced mg metal matrix composites brake calliper: simulation approach. In: *Proc. of 4th International Conference on Mechanical Engineering Research (ICMER2017)*. 2017.
  25. Salim SM, Cheah SC. Wall  $y^+$  Strategy for Dealing with Wall-bounded Turbulent Flows. In: *Proc. of Proceedings of the International MultiConference of Engineers and Computer Scientists, Hong Kong*. 2009.